Conformational Analysis of Oligothiophenes and Oligo(thienyl)furans by Use of a Combined Molecular Dynamics/NMR Spectroscopic Protocol

Gerardo A. Diaz-Quijada,[†] Noham Weinberg,[†,‡] Steven Holdcroft,*[,†] and B. Mario Pinto*[,†]

Department of Chemistry, Simon Fraser University, Burnaby, B.C., Canada, V5A 1S6, and Department of Chemistry, University College of the Fraser Valley, Abbortsford, B.C., Canada, V2S 7M8

Received: May 10, 2001; In Final Form: August 7, 2001

The conformational analysis of oligothiophenes and oligo(thienyl)furans by use of a combined molecular dynamics (MD)/NMR spectroscopic protocol is described. A series of MD simulations were performed for 2-(2′-thienyl)-3-hexylthiophene (**2**), 2,5-bis(3′-hexyl-2′-thienyl)thiophene (**3**), 2,5-bis(4′-hexyl-2′-thienyl)-thiophene (**4**), 2,5-bis(3′-hexyl-2′-thienyl)furan (**5**), and 2,5-bis(4′-hexyl-2′-thienyl)furan (**6**) with a new MM2 torsional parameter set developed earlier for unsubstituted and methyl-substituted 2,2′-bithiophene and 2-(2′-thienyl)furan systems. Conformationally averaged structures were determined for each of these molecules. Theoretical NOE buildup curves were then calculated for these averaged structures using a full matrix relaxation treatment and were compared to those obtained experimentally. Excellent agreement between the calculated and experimental NOE buildup curves was generally observed, in particular for the 2,2′-bithiophene systems.

Introduction

Conjugated polymers have been the subject of intense research[1,2] since the first observation of electrical conductivity in polyacetylene[3] in its oxidized form. More recently, research on conjugated polymers has focused on their luminescent properties.[4] Polythiophenes have attracted a great deal of attention due to their high chemical and electrochemical stability in their neutral and oxidized states.[1,5] The unsubstituted polythiophene is insoluble and intractable, and this prevents not only extensive characterization of the material but also its potential application in the fabrication of devices. Substitution at the 3-position, however, produced materials that are soluble in common organic solvents[6−8] and even in water.[9]

Although substituted polythiophenes have been considered to be potential candidates for luminescent devices, substituted poly(thienyl)furans were found to exhibit even higher photoluminescent quantum yields.[10] This enhanced efficiency has been attributed to the fact that sulfur is replaced with a lighter atom (oxygen) in the polymer chain. Heavy atoms increase the probability for intersystem crossing, thereby decreasing the quantum yield in photoluminescence.[11]

Since the electrical and luminescent properties in conjugated polymers are directly affected by the overlap of p orbitals, resulting in conjugation along the polymer chain, further advances in the design of new materials require a deeper understanding of the dynamics of the conformational properties in these systems.

A number of theoretical[12−42] and experimental[17−21,32,40−51] studies of conformations of oligo- and polythiophenes has been reported. Although X-ray crystallographic studies[18,20,21,43,45−48] indicate that these compounds might be planar in the solid state, studies in solution indicate that they are substantially nonplanar.[40−42] Similarly, ab initio calculations performed at Hartree−Fock, DFT, and MP2 levels with various basis sets ranging from 3-21G* to 6-311G** consistently indicate that cis and trans conformers are nonplanar.[17,35−42]

CHART 1

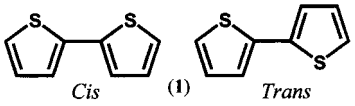

Our ab initio and dynamic NMR studies[52] indicate that the torsional barriers in oligothiophenes and oligo(thienyl)furans are low and thus a rapid interconversion between the conformers is expected. Substitution at the 3-position decreases the energy barrier for cis-trans interconversion since steric interactions destabilize the stable conformers (cis and trans) with respect to the 90° -twisted transition state. At the same time, as expected, the energy barrier for the interconversion between the cis and its cis-mirror image conformer increases since this process requires passage through the fully coplanar, sterically hindered cis transition state. The same is true for the exchange between the trans conformer and its mirror image. The steric effect is so pronounced for ethyl and longer alkyl substituents that the energy barrier between cis and trans conformers virtually disappears, and these conformations can no longer be differentiated.

The present work provides further insight into the dynamics of the conformational behavior of these systems by comparison of the results of nuclear Overhauser effect (NOE) measurements and constant temperature molecular dynamics (MD) simulations. The MD simulations make use of the new MM2 parameter set developed in our earlier work.[52]

Experimental Section

The syntheses of the substituted trimers[10] and 2-(2′-thienyl)-3-hexylthiophene (**2**)[52] have been published previously. NMR samples were prepared by dissolving approximately 5 mg of the desired compound in $CDCl_3$. These solutions were subsequently degassed via three freeze−pump−thaw cycles and then sealed under nitrogen. Chemical shifts are referenced to tetramethylsilane ($\delta = 0$ ppm). NMR experiments, unless other-

* Corresponding authors. S.H.: e-mail, holdcrof@sfu.ca; tel, (604)-291-4221; fax, (604)-291-3765. B.M.P.: e-mail, bpinto@sfu.ca; tel, (604)-291-4884; fax, (604)-291-5424.

[†] Simon Fraser University.

[‡] University College of the Fraser Valley.

10.1021/jp011784l CCC: $22.00
Published on Web 01/30/2002

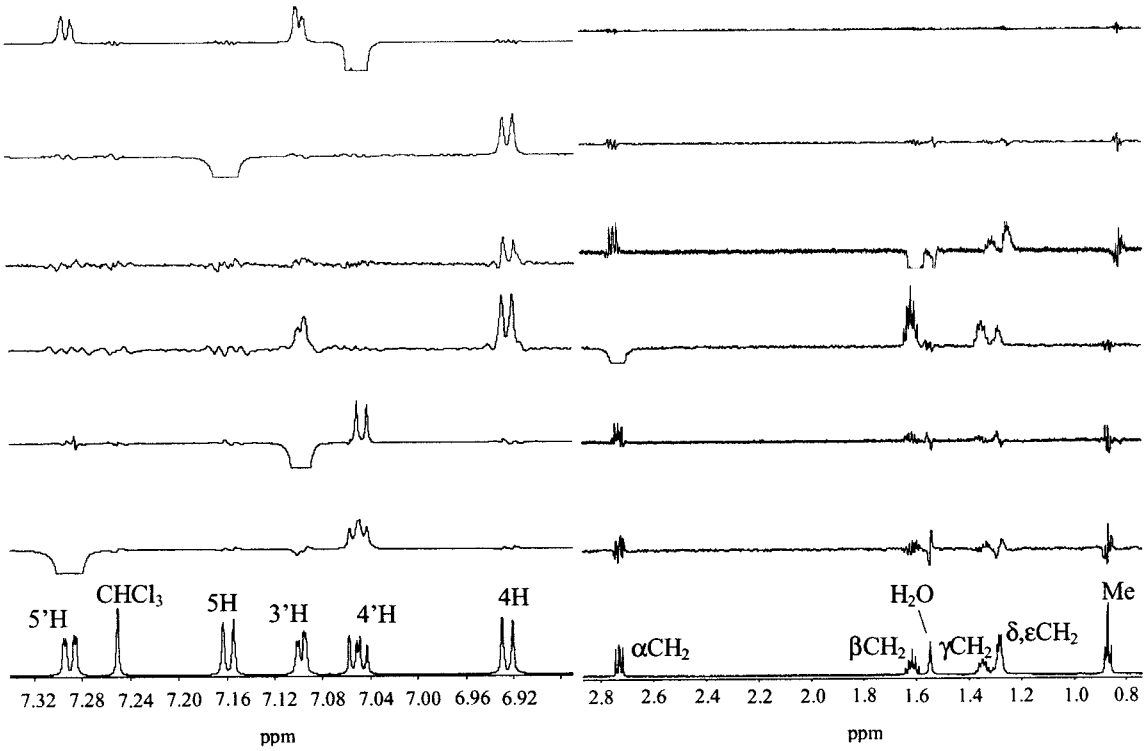

Figure 1. Transient 1D-NOE spectra for 2-(2′-thienyl)-3-hexylthiophene (**2**). The bottom spectrum corresponds to the control experiment.

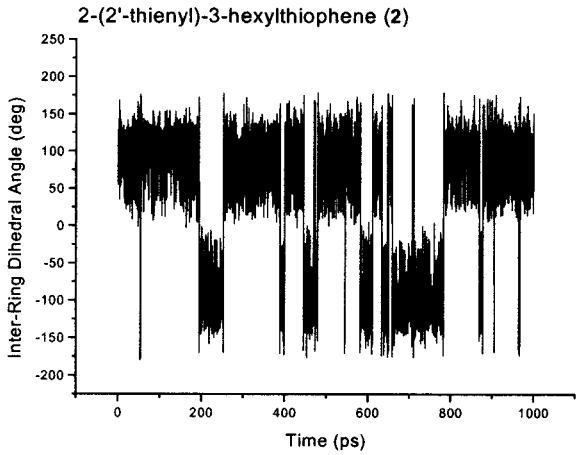

Figure 2. Inter-ring dihedral angle as a function of time during the dynamics simulation for 2-(2′-thienyl)-3-hexylthiophene (**2**).

wise stated, were acquired on an AMX600 Bruker instrument operating at 600.13 MHz and 298 K.

The 1D transient NOE experiments were performed by inverting the signal of interest with a 200ms Gaussian selective pulse which was constructed from 1024 steps. Spectra were collected in difference mode by alternating the phase of the receiver gain during on- and off-resonance. The digitized signal was stored in an 8 K data set using a sweep width of 10.33 ppm, an acquisition time of 0.496 s, 512 scans, and 4 dummy scans. Processing of the spectra was accomplished by zero filling to 32 K followed by an exponential multiplication using a line width of 1 Hz. All integrals were obtained after careful phase and baseline correction. Fractional NOEs were calculated as the area ratio of the enhanced and the inverted signals. All NOE enhancements were subsequently divided by the extrapolated area of the inverted signal at zero time. This ensures that the enhancements are corrected for zero mixing time. Extrapolation was performed by fitting the area of the inverted signal as a function of mixing time to an exponential function.

Computations

Molecular dynamics simulations were performed on an Indigo Silicon Graphics workstation running Tinker version 3.6[53] using the MM2(91) force field with a modified set of torsional parameters[52] and the default dielectric constant of 1.5. All dynamics simulations were carried out with an integration step of 0.5 fs in 500 ps runs, except for the simulation of 2-(2′-thienyl)-3-hexylthiophene (**2**), which was twice as long. Atomic coordinates were stored every 0.1 ps to give a total of 5000 (10000 for 2-(2′-thienyl)-3-hexylthiophene (**2**)) coordinate frames along a dynamics trajectory. The coupling time for the temperature bath was set to 0.01 ps in all cases. The equilibration time for each run was assessed graphically from the time dependencies of the temperature and kinetic, potential, and total energy of the system. In all cases, equilibration was attained within the first 10 ps of the simulation. The average internuclear distances were evaluated as $\langle r^{-6}\rangle^{-1/6}$ and $\langle r^{-3}\rangle^{-1/3}$:

$$\langle r^{-6}\rangle^{-1/6} = \left[\frac{1}{M}\sum_{u=1}^{M} r_u^{-6}\right]^{-1/6} \quad (1)$$

Here, r_u is an inter-nuclear distance at instant t_u, and M is

$$\langle r^{-3}\rangle^{-1/3} = \left[\frac{1}{M}\sum_{u=1}^{M} r_u^{-3}\right]^{-1/3} \quad (2)$$

the number of frames along a molecular dynamics trajectory.

Calculations of the NOE buildup curves were performed with a modified version of CROSREL (version 3.56).[54] The best correlation time and leakage rate for each individual pair of observed NMR signals was obtained via a grid search method. The optimized parameters were employed in the calculation of the theoretical NOE buildup curves.

Results and Discussion

A series of molecular dynamics simulations were carried out to produce conformationally averaged structures of compounds

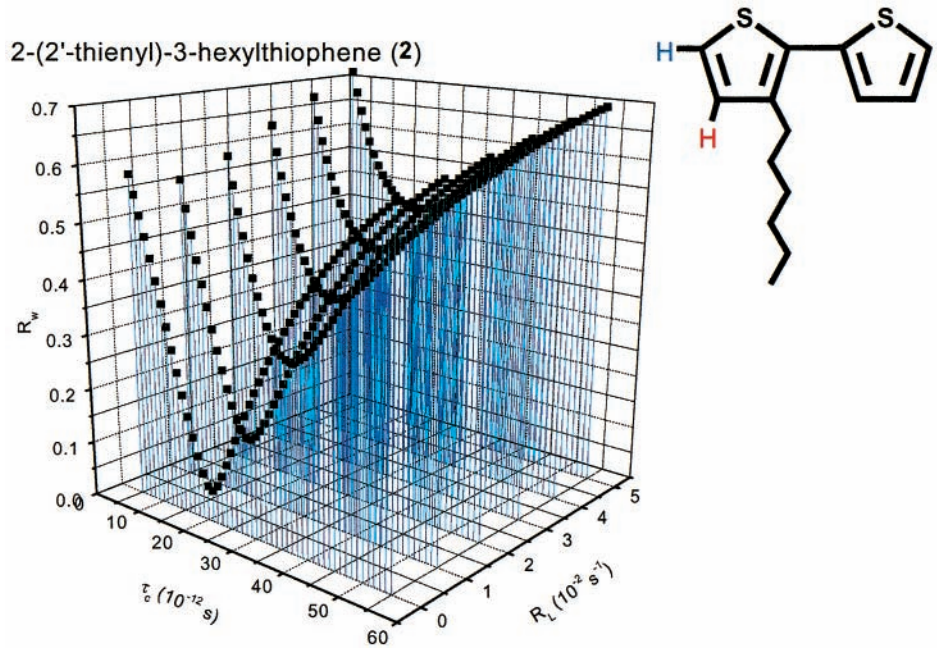

Figure 3. Typical plot of the grid search results for determining the optimum values of the correlation time (τ_c) and the leakage rate (R_L) for a particular set of protons. In this example with 2-(2′-thienyl)-3-hexylthiophene (**2**), the NOE at 4H is observed when the signal from 5H is inverted.

CHART 2

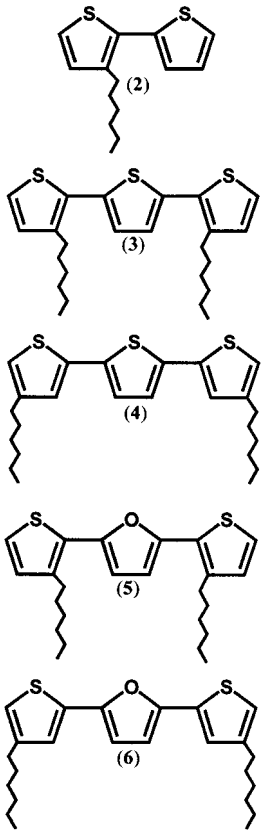

2−**6**. Theoretical NOE buildup curves were then calculated from these averaged structures using a full relaxation matrix approach and compared to the experimental NOE buildup curves. The protocol is illustrated in detail for the case of 2-(2′-thienyl)-3-hexylthiophene (**2**); the results for the remaining compounds **3**−**6** then follow.

2-(2′-Thienyl)-3-hexylthiophene (2). Several 1D-NOESY spectra were collected as a function of mixing time. Complete buildups and decays were acquired in most cases. Sample spectra, as well as the control spectrum, are presented in Figure 1.

Molecular dynamics simulations consisted of 1000 ps runs, with the first 10 ps allowed for equilibration. A plot of the inter-ring dihedral angle as a function of time (Figure 2) clearly indicates that the conformational space was sampled adequately.

The mean inter-proton distances obtained from the trajectories, averaged as $\langle r^{-6}\rangle^{-1/6}$ (eq 1), were used to calculate the theoretical NOE spectra at different mixing times. It was assumed in this case that motional averaging is slow on the molecular tumbling time scale. The correlation time, τ_c, and the leakage rate, R_L were obtained by minimization of the weighted residual factor, R_w, a quantitative measure of the differences between the theoretical and experimental NOE buildup curves. Figure 3 illustrates the behavior of R_w as a function of τ_c and R_L. It is important to note that this function possessed a single minimum.

The experimental and theoretical NOE buildup curves calculated using the optimized τ_c and R_L parameters are compared in Figure 4. Excellent agreement obtained between the theoretical and experimental curves for the NOE contacts from proton sets in the rigid part of the molecule (Figure 4a−4e) illustrates the quality of the computational protocol. Equally good agreement obtained for the NOE contacts between 3′H and αCH_2 (Figure 4f,g) demonstrates the reliability of the MD simulation of the inter-ring torsion.

A somewhat poorer agreement observed for the NOE contacts between methylene protons in the alkyl chain (Figure 4h−k) and between the aromatic and the methylene protons (Figure 4l,m) should probably be attributed to a poorer parametrization of MM2 for torsions in alkyl substituents on thiophenes.

The curves in Figure 4f,g are due to the contacts between 3′H and αCH_2 protons, and therefore, they provide a probe of the inter-ring internal motion. Averaging the inter-proton distances as $\langle r^{-6}\rangle^{-1/6}$ (eq 1) implies that the inter-ring torsional motion occurs slower than the overall molecular tumbling. It is therefore of interest to compare the experimental NOE buildup curves to those obtained from averaging distances as $\langle r^{-3}\rangle^{-1/3}$ (eq 2), which would represent the case of inter-ring torsion that

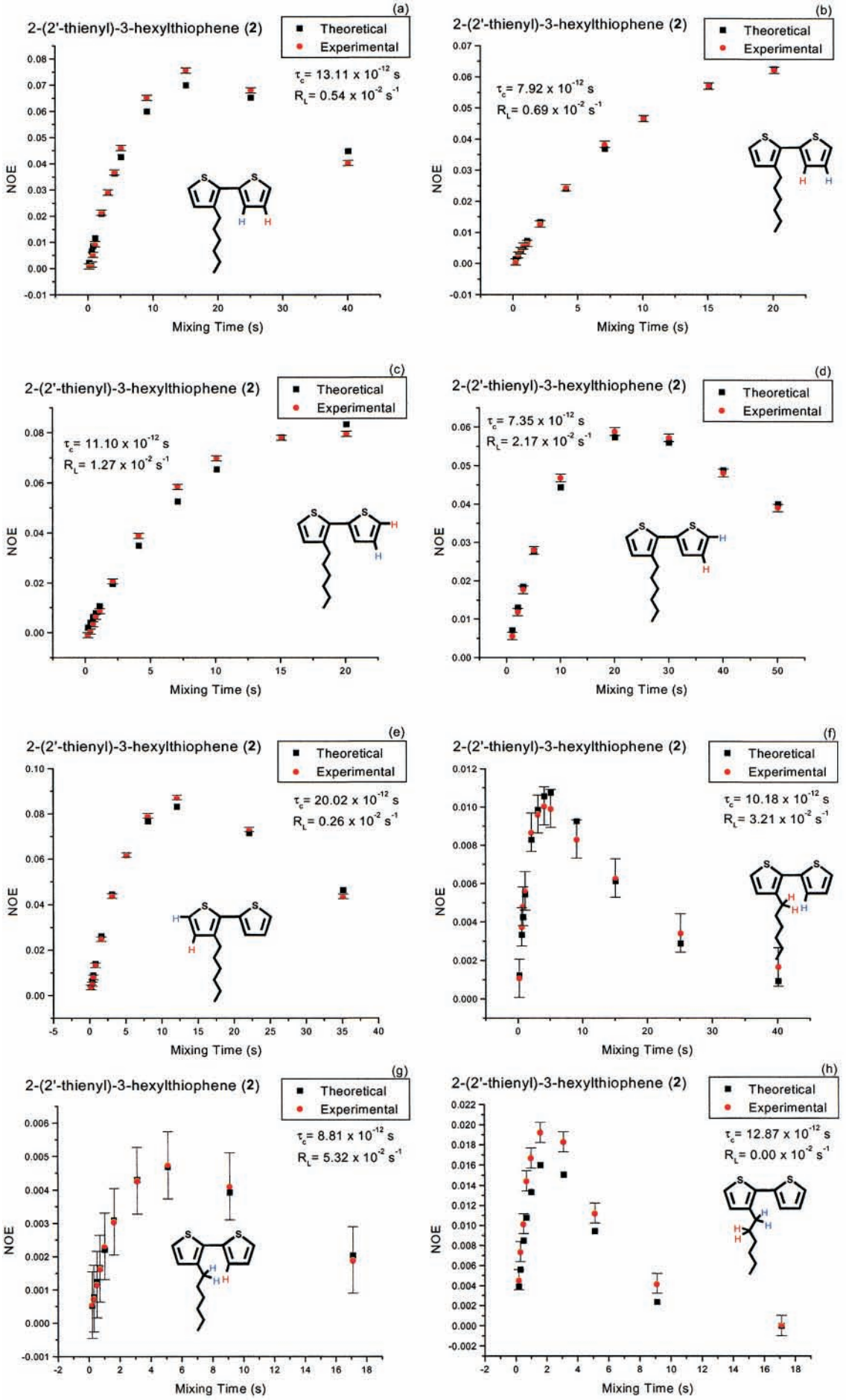
(a)
2-(2'-thienyl)-3-hexylthiophene (2)
Theoretical
Experimental
τ_c= 13.11 x 10^{-12} s
R_L= 0.54 x 10^{-2} s^{-1}
NOE
Mixing Time (s)
(b)
2-(2'-thienyl)-3-hexylthiophene (2)
Theoretical
Experimental
τ_c= 7.92 x 10^{-12} s
R_L= 0.69 x 10^{-2} s^{-1}
NOE
Mixing Time (s)
(c)
2-(2'-thienyl)-3-hexylthiophene (2)
Theoretical
Experimental
τ_c= 11.10 x 10^{-12} s
R_L= 1.27 x 10^{-2} s^{-1}
NOE
Mixing Time (s)
(d)
2-(2'-thienyl)-3-hexylthiophene (2)
Theoretical
Experimental
τ_c= 7.35 x 10^{-12} s
R_L= 2.17 x 10^{-2} s^{-1}
NOE
Mixing Time (s)
(e)
2-(2'-thienyl)-3-hexylthiophene (2)
Theoretical
Experimental
τ_c= 20.02 x 10^{-12} s
R_L= 0.26 x 10^{-2} s^{-1}
NOE
Mixing Time (s)
(f)
2-(2'-thienyl)-3-hexylthiophene (2)
Theoretical
Experimental
τ_c= 10.18 x 10^{-12} s
R_L= 3.21 x 10^{-2} s^{-1}
NOE
Mixing Time (s)
(g)
2-(2'-thienyl)-3-hexylthiophene (2)
Theoretical
Experimental
τ_c= 8.81 x 10^{-12} s
R_L= 5.32 x 10^{-2} s^{-1}
NOE
Mixing Time (s)
(h)
2-(2'-thienyl)-3-hexylthiophene (2)
Theoretical
Experimental
τ_c= 12.87 x 10^{-12} s
R_L= 0.00 x 10^{-2} s^{-1}
NOE
Mixing Time (s)

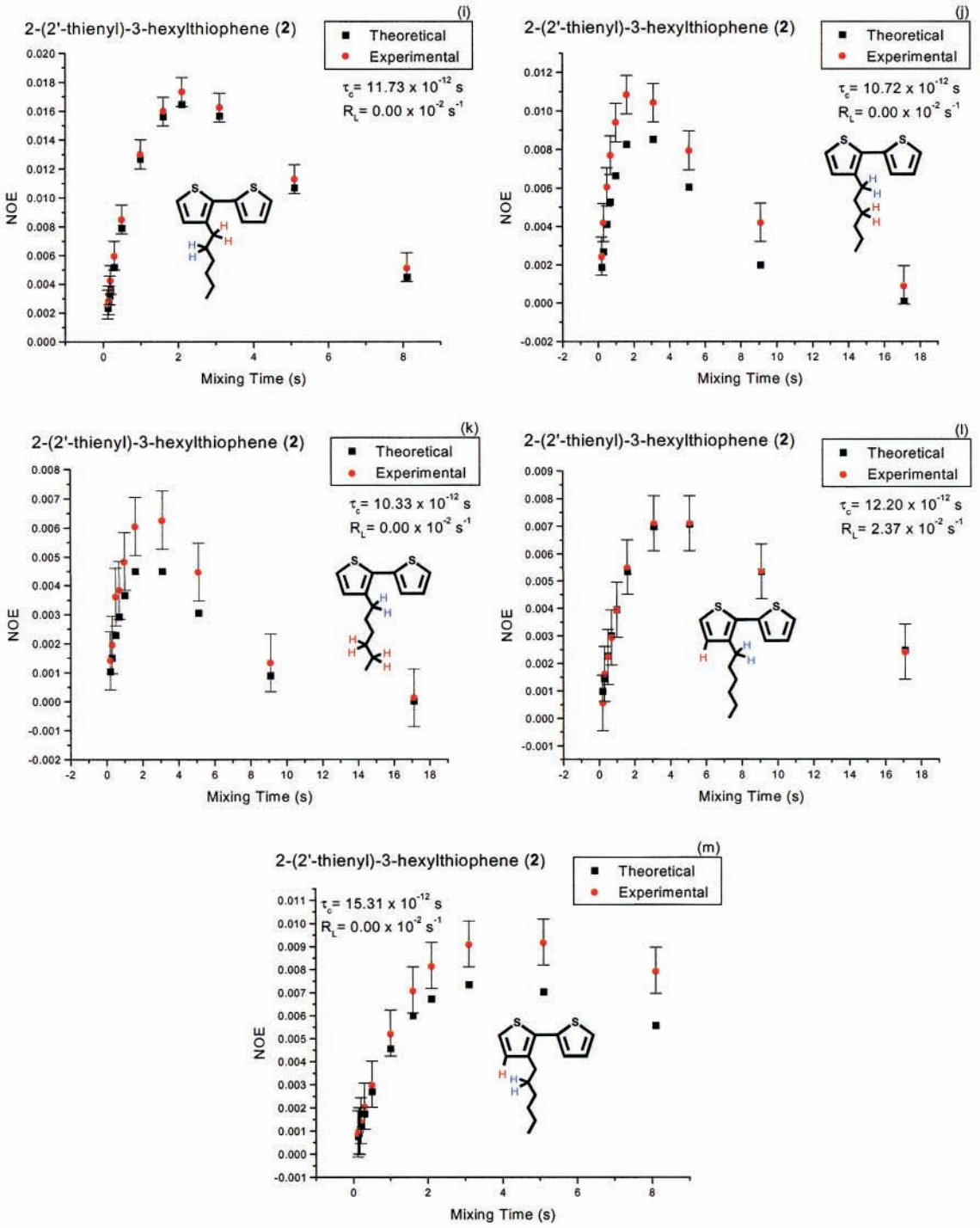

Figure 4. Experimental and theoretical NOE buildup curves for various proton sets in 2-(2′-thienyl)-3-hexylthiophene (**2**). These theoretical NOE curves were obtained by averaging interproton distances from a molecular dynamics simulation as $\langle r^{-6}\rangle^{-1/6}$. The observed and inverted proton resonances are depicted in red color and blue color, respectively.

is faster than the overall molecular tumbling. The relevant curves are shown in Figure S1 (Supporting Information). The comparison of Figure 4f,g and Figure S1f,g clearly demonstrates that the $\langle r^{-6}\rangle^{-1/6}$ averaging produces much better results than the $\langle r^{-3}\rangle^{-1/3}$ scheme, which indicates that the inter-ring torsion in 2-(2′-thienyl)-3-hexylthiophene (**2**) is slower than the overall molecular tumbling.

Oligothiophenes and Oligo(thienyl)furans 3−6. The dynamic study described in the preceding section for 2-(2′-thienyl)-3-hexylthiophene (**2**) was extended to 2,5-bis(3′-hexyl-2′-thienyl)thiophene (**3**), 2,5-bis(4′-hexyl-2′-thienyl)thiophene (**4**), 2,5-bis(3′-hexyl-2′-thienyl)furan (**5**), and 2,5-bis(4′-hexyl-2′-thienyl)furan (**6**). Representative NMR spectra for these compounds are presented in Figures 5−8. Molecular dynamics simulations were performed as described above in a series of 500 ps runs with 10ps equilibration periods. The dynamics of internal rotation in these systems is represented by the graphs in Figures 9−12. As is evident from the figures, the dynamic behavior of (**3**) (Figure 9) is quite similar to that of (**2**) (Figure 2). The system oscillates freely between its cis and trans conformations but needs to overcome a barrier to proceed through coplanar states. The motion is strongly coupled

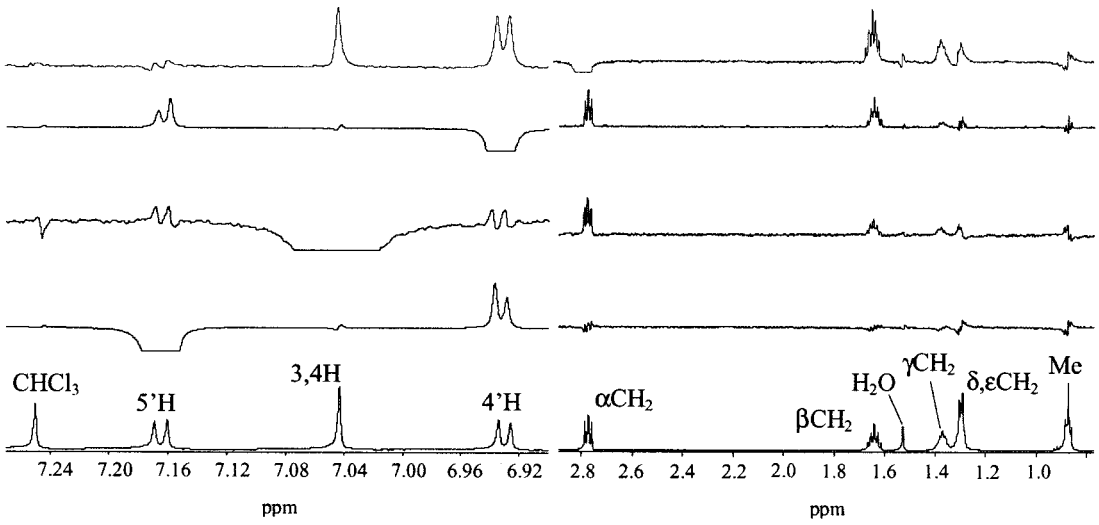

Figure 5. Transient 1D-NOE spectra for 2,5-bis(3′-hexyl-2′-thienyl)thiophene (**3**). The bottom spectrum corresponds to that from the control experiment.

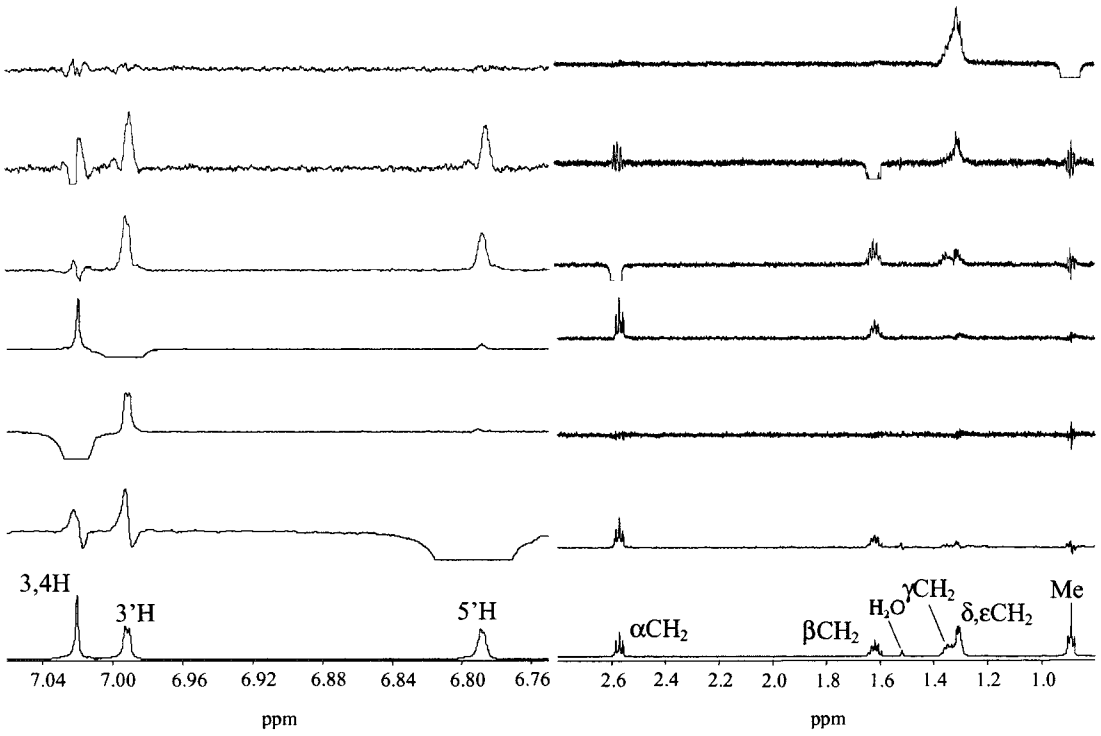

Figure 6. Transient 1D-NOE spectra for 2,5-bis(4′-hexyl-2′-thienyl)thiophene (**4**). The bottom spectrum corresponds to that from the control experiment.

since the two inter-ring torsion angles tend to have opposite signs in order to minimize the steric repulsion and preserve total angular momentum. The barriers are lower in **4**−**6** and, therefore, can be readily overcome, as evident from Figures 10−12.

Theoretical and experimental NOE buildup curves for compounds **3**−**6** are compared in Figures S2−S7 (Supporting Information). Excellent agreement is generally obtained for most proton pairs, although only reasonable agreement is obtained in the cases of the contacts between (i) the αCH_2 protons on C-3 and the inter-ring 3′H in compound (**3**) (Figures S3c-S3f), (ii) the αCH_2 protons on C-4 and the same-ring 3H in compound (**4**) (Figures S4i, S4j), (iii) the βCH_2 protons on C-4 and the same-ring 3H in compound (**4**) (Figure S4n), (iv) the αCH_2 protons on C-3 and the inter-ring 3H in compound (**5**) (Figures S6d, S6e), and (v) the βCH_2 protons on C-3′ and the inter-ring 3H in compound (**5**) (Figure S6g). In contrast, extremely poor agreement is obtained for the contacts between the αCH_2 and βCH_2 protons on C-4′ and the inter-ring furan 3H and 4H in compound (**6**) (panels d and e, respectively, of Figure S7). Excellent agreement between experimental and theoretical curves for the inter-ring 3H′ and 3H protons in this compound (Figure S7b,c) shows the reliability of the MD simulatons of the inter-ring torsion. We therefore attribute the discrepancies observed in Figure S7d,e to the inaccurate modeling of the torsional behavior of alkyl substituents on thiophene rings by the original MM2 parameter set.

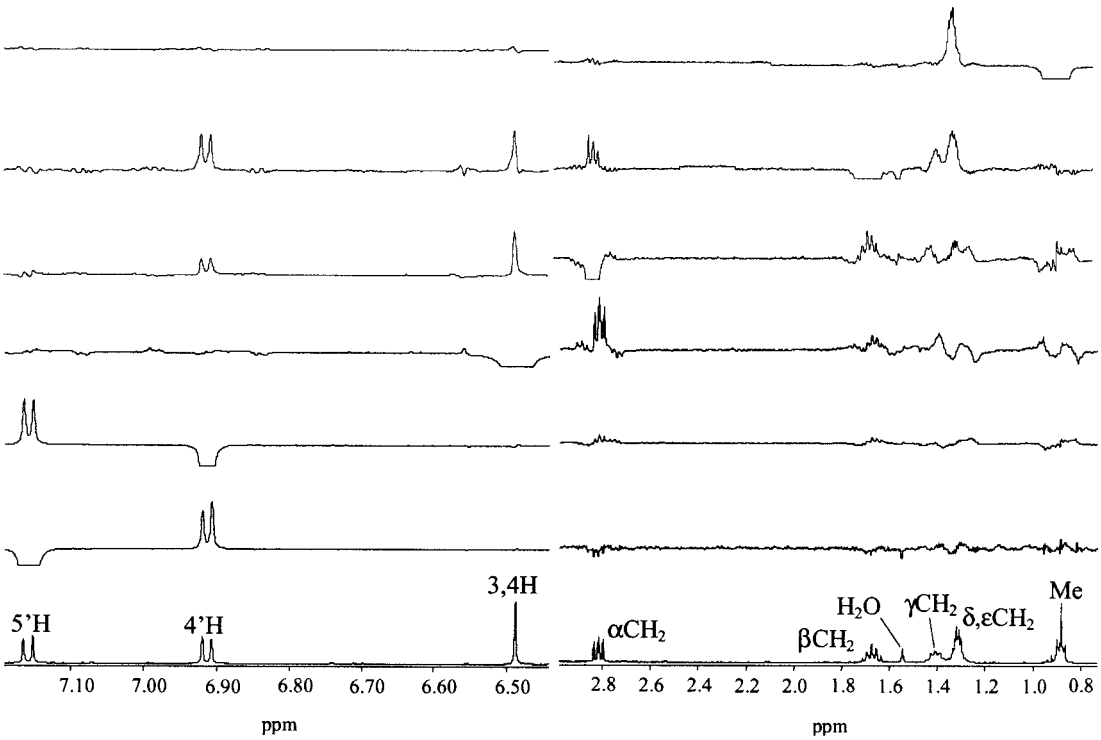

Figure 7. Transient 1D-NOE spectra for 2,5-bis(3′-hexyl-2′-thienyl)furan (**5**). The bottom spectrum corresponds to that from the control experiment.

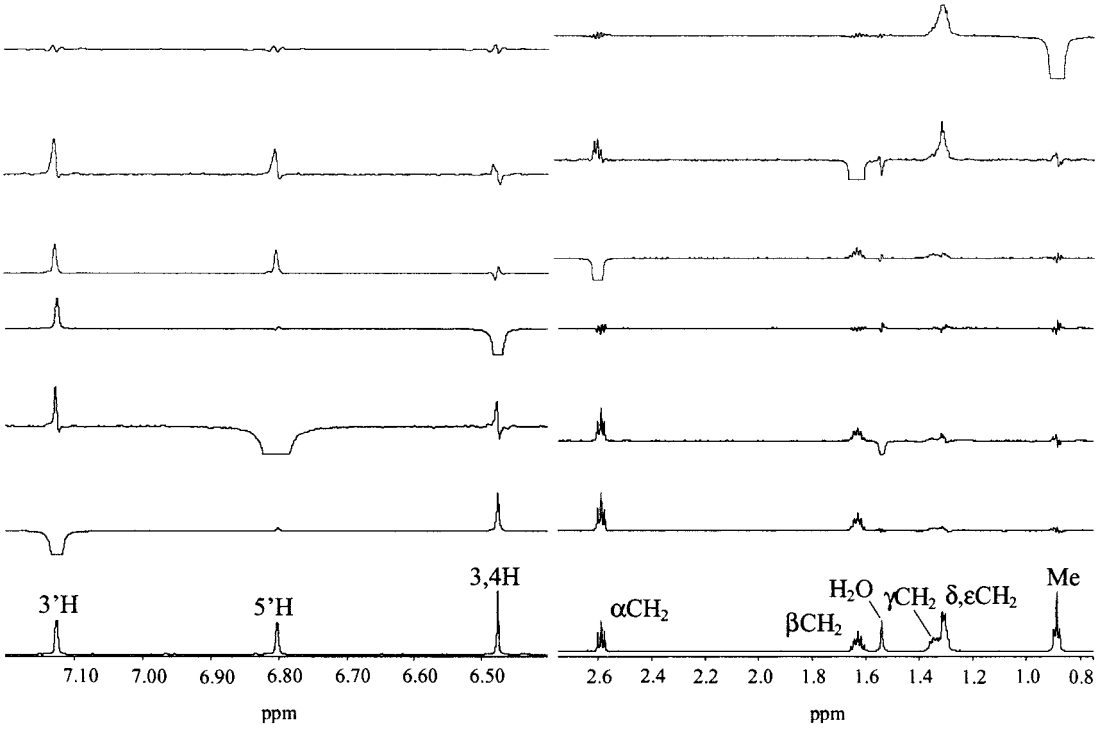

Figure 8. Transient 1D-NOE spectra for 2,5-bis(4′-hexyl-2′-thienyl)furan (**6**). The bottom spectrum corresponds to that from the control experiment.

Conclusions

The new parameter set for the MM2 force field, developed in our earlier work,[52] accurately predicted the conformational properties of 2-(2′-thienyl)-3-hexylthiophene (**2**), 2,5-bis(3′-hexyl-2′-thienyl)thiophene (**3**), 2,5-bis(4′-hexyl-2′-thienyl)thiophene (**4**), 2,5-bis(3′-hexyl-2′-thienyl)furan (**5**) and 2,5-bis(4′-hexyl-2′-thienyl)furan (**6**). Thus, NOE buildup curves calculated from average conformations obtained from molecular dynamics simulations, gave excellent or very good agreement with experimentally derived curves for almost all proton pairs. The $\langle r^{-6}\rangle^{-1/6}$ averaging scheme for inter-proton distances provided a better fit with experimental data than the $\langle r^{-3}\rangle^{-1/3}$ scheme, suggesting that internal motion occurs at a lower rate than the overall molecular tumbling.

Although the new parameter set was developed for methyl-substituted molecules containing two heterocyclic rings, it provides an excellent model for the hexyl-substituted tricyclic systems **2**−**6**, and this is expected to hold true for

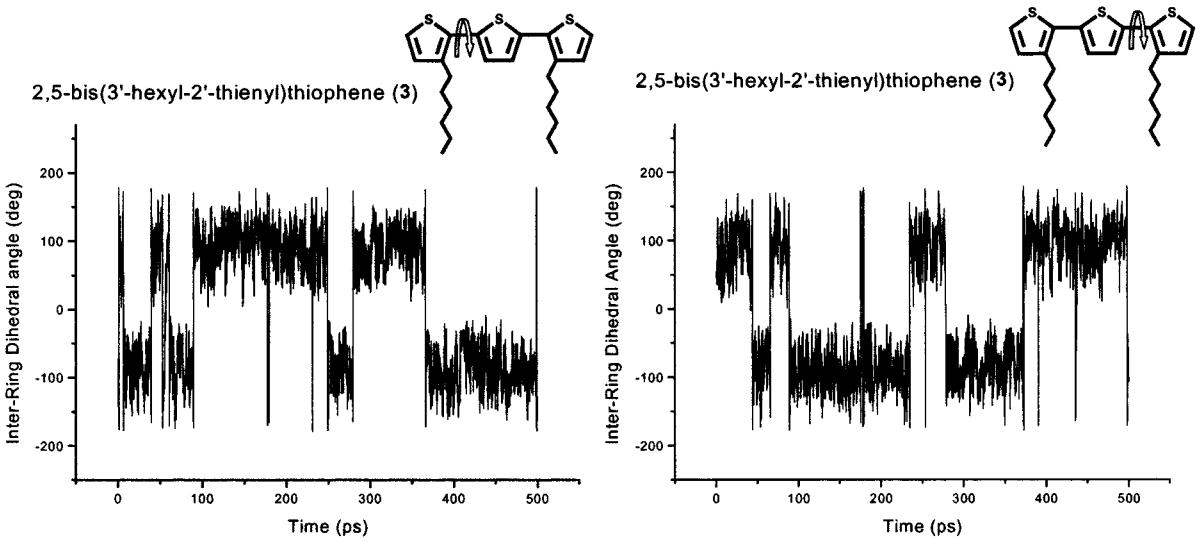

Figure 9. Inter-ring dihedral angles for each torsion between the thiophene rings as a function of time during the dynamics simulation of 2,5-bis(3′-hexyl-2′-thienyl)thiophene (**3**).

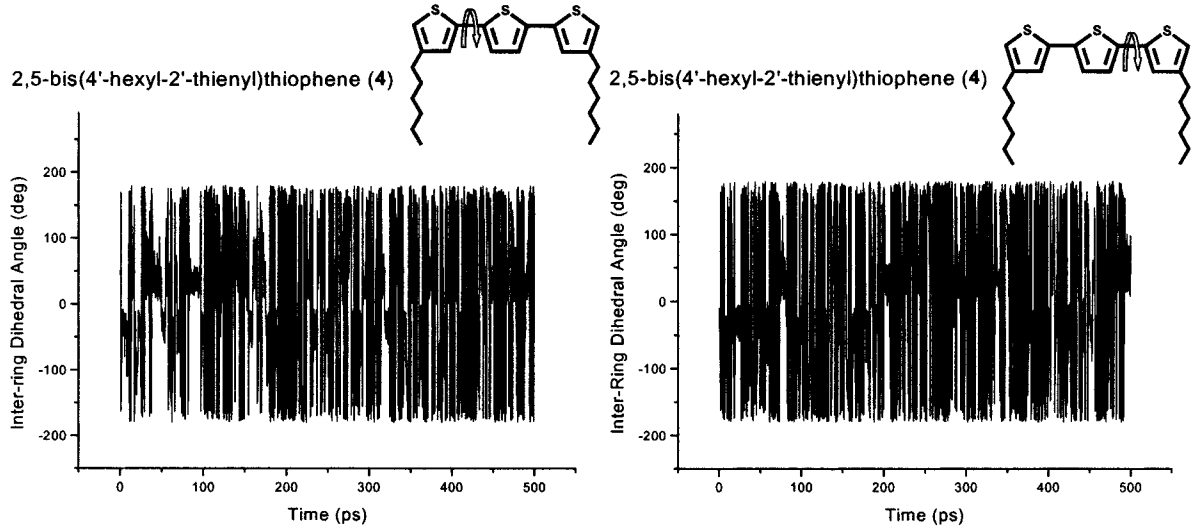

Figure 10. Inter-ring dihedral angles as a function of time for 2,5-bis(4′-hexyl-2′-thienyl)thiophene (**4**).

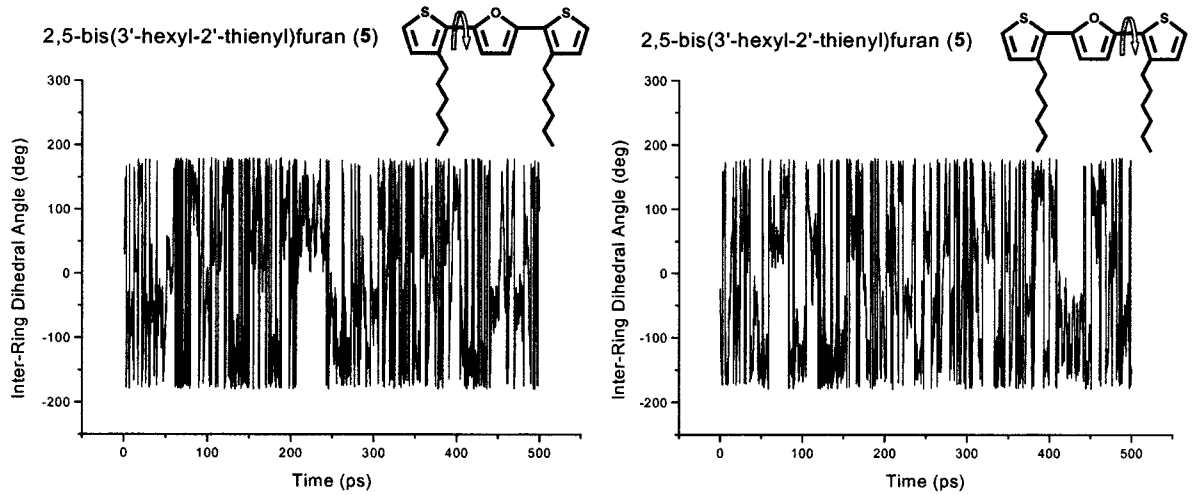

Figure 11. Inter-ring dihedral angles as a function of time for 2,5-bis(3′-hexyl-2′-thienyl)furan (**5**).

alkyl substituents of different lengths. The new MM2 torsional parameter set models accurately the dynamics of conformational exchange in oligothiophenes and oligo(thienyl)-furans, and it should, therefore, permit the study of the conformational properties of longer oligomers and perhaps even polymers.

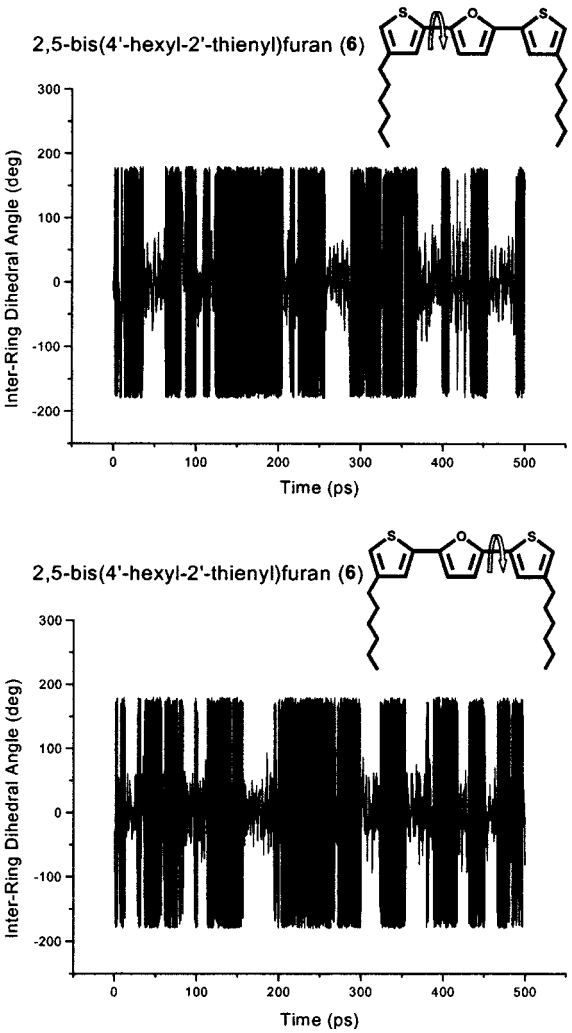

Figure 12. Inter-ring dihedral angles as a function of time for 2,5-bis(4′-hexyl-2′-thienyl)furan (**6**).

Acknowledgment. We are grateful to the Natural Sciences and Engineering Research Council of Canada for financial support and to J. Borwein for access to his computational facilities.

Supporting Information Available: Theoretical and experimental NOE buildup curves for 2-(2′-thienyl)-3-hexylthiophene (**2**), 2,5-bis(3′-hexyl-2′-thienyl)thiophene (**3**), 2,5-bis(4′-hexyl-2′-thienyl)thiophene (**4**), 2,5-bis(3′-hexyl-2′-thienyl)furan (**5**), and 2,5-bis(4′-hexyl-2′-thienyl)furan (**6**). This material is available free of charge via the Internet at http://pubs.acs.org.

References and Notes

(1) Roncali, J. *Chem. Rev.* **1992**, *92*, 711.
(2) Skotheim, B. *Handbook of Conducting Polymers*; Marcel: New York, 1986; Vols. 1 and 2.
(3) Shirakawa, H.; Louis, E. J.; MacDiarmid, A. G.; Chiang, C. K.; Heeger, A. J. *J. Chem. Soc., Chem. Commun.* **1977**, 578.
(4) Tourillon, G. In *Polythiophene and Its Derivatives*; Tourillon, G., Ed.; Marcel Dekker: New York, 1986; Vol. 1, p 293.
(5) Burroughes, J. H.; Bradley, D. D. C.; Brown, A. R.; Marks, R. N.; Mackay, K.; Friend, R. H.; Burn, P. L.; Holmes, A. B. *Nature* **1990**, *347*, 539.
(6) Hotta, S.; Rughooputh, S. D. D. V.; Heeger, A. J.; Wudl, F. *Macromolecules* **1987**, *20*, 212.
(7) Elsenbaumer, R. L.; Jen, K. Y.; Oboodi, R. *Synth. Met.* **1986**, *15*, 169.
(8) Sato, M.; Tanaka, S.; Kaeriyama, K. *J. Chem. Soc., Chem. Commun.* **1986**, 873.
(9) Patil, A. O.; Ikenone, Y.; Wudl, F.; Heeger, A. *J. Am. Chem. Soc.* **1987**, *109*, 1858.
(10) Yang, C.; Abley, M.; Holdcroft, S. *Macromolecules* **1999**, *32*, 6889.
(11) Saadeh, H.; Goodson, T.; Yu, L. *Macromolecules* **1997**, *30*, 4608.
(12) Barbarella, G.; Bongini, A.; Zambianci, M. *Adv. Mater.* **1991**, *3*, 494.
(13) Bredas, J. L.; Heeger, A. J. *Macromolecules* **1990**, *23*, 1150.
(14) Kofranek, M.; Kovar, T.; Lischka, H.; Karpfen, A. *J. Mol. Struct.* **1992**, *259*, 181.
(15) Salzner, U.; Lagowski, J. B.; Pickup, P. G.; Poirier, R. A. *Synth. Met.* **1998**, *96*, 177.
(16) Bredas, J. L.; Street, G. B.; Themans, B.; Andre, J. M. *J. Chem. Phys.* **1985**, *83*, 1323.
(17) Samdal, S.; Samuelsen, E. J.; Volden, H. V. *Synth. Met.* **1993**, *59*, 259.
(18) Barbarella, G.; Zambianchi, M.; Bongini, A.; Antolini, L. *Adv. Mater.* **1992**, *4*, 282.
(19) Barbarella, G.; Bongini, A.; Zambianchi, M. *Tetrahedron* **1992**, *48*, 6701.
(20) Barbarella, G.; Zambianchi, M.; Bongini, A.; Antolini, L. *Adv. Mater.* **1993**, *5*, 834.
(21) Barbarella, G.; Zambianchi, M.; Antolini, L.; Folli, U.; Goldoni, F.; Iarossi, D.; Schenetti, L.; Bongini, A. *J. Chem. Soc., Perkin Trans. 2* **1995**, 1869.
(22) Arbizzani, C.; Barbarella, G.; Bongini, A.; Mastragostino, M.; Zambianchi, M. *Synth. Met.* **1992**, *52*, 329.
(23) Hernandez, V.; Lopez Navarrete, J. T. *J. Chem. Phys.* **1994**, *101*, 1369.
(24) Hernandez, V.; Ramirez, F. J.; Casado, J.; Enriques, F.; Quirante, J. J.; Lopez Navarrete, J. T. *J. Mol. Struct.* **1997**, *410−411*, 311.
(25) Barone, V.; Lelj, F.; Russo, N.; Toscano, M. *J. Chem. Soc., Perkin Trans. 2* **1986**, 907.
(26) Subramanian, H.; Lagowski, J. B. *Int. J. Quantum Chem.* **1998**, *66*, 229.
(27) Di Césare, N.; Belletête, M.; Leclerc, M.; Durocher, G. *Synth. Met.* **1998**, *94*, 291.
(28) Distefano, G.; Colle, M. D.; Jones, D.; Zambianchi, M.; Favaretto, L.; Modelli, A. *J. Phys. Chem.* **1993**, *97*, 3504.
(29) Skancke, A. *Acta Chem. Scand.* **1970**, *24*, 1389.
(30) Galasso, V.; Trinajstic, N. *Tetrahedron* **1972**, *28*, 4419.
(31) Bongini, A.; Brioni, F.; Panunzio, M. *J. Chem. Soc., Perkin Trans 2* **1997**, 927.
(32) Belletête, M.; Leclerc, M.; Durocher, G. *J. Phys. Chem.* **1994**, *98*, 9450.
(33) dos Santos, D. A.; Galvao, D. S.; Laks, B.; dos Santos, M. C. *Chem. Phys. lett.* **1991**, *184*, 579.
(34) Di Césare, N.; Belletête, M.; Durocher, G.; Leclerc, M. *Chem. Phys. Lett.* **1997**, *275*, 533.
(35) Samdal, S.; Samuelson, E. J.; Volden, H. V. *Synth. Met.* **1993**, *59*, 259.
(36) Ortí, E.; Viruela, P. M.; Sánchez-Marin, J.; Tomás, F. *J. Phys. Chem.* **1995**, *99*, 4955.
(37) Ciofalo, M.; La Manna, G. *Chem. Phys. Lett.* **1996**, *263*, 73.
(38) Alemán, C.; Julia, L. *J. Phys. Chem.* **1996**, *100*, 1524.
(39) Bongini, A.; Bottoni, A. *J. Phys. Chem. A* **1999**, *103*, 6800.
(40) Di Césare, N.; Belletête, M.; Raymond, F.; Leclerc, M.; Durocher, G. J. *Chem. Phys. A.* **1998**, *102*, 2700.
(41) Di Césare, N.; Belletête, M.; Marrano, C.; Leclerc, M.; Durocher, G. J. *Chem. Phys. A.* **1998**, *102*, 5142.
(42) Di Césare, N.; Belletête, M.; Leclerc, M.; Durocher, G. J. *Chem. Phys. A* **1999**, *103*, 803.
(43) Visser, G. J.; Heeres, G. J.; Wolters, J.; Vos, A. *Acta Crystallogr.* **1968**, *B24*, 467.
(44) Bucci, P.; Longeri, M.; Veracini, C. A.; Lunazzi, L. *J. Am. Chem. Soc.* **1974**, *96*, 1305.
(45) Delugeard, Y.; Desuche, J.; Baudour, J. L. *Acta Crystallogr.* **1976**, *B32*, 702.
(46) Baudour, J. L.; Delugeard, Y.; Rivet, P. *Acta Crystallogr.* **1978**, *B34*, 625.
(47) Hotta, S.; Waragai, K. *Adv. Mater.* **1993**, *5*, 896.
(48) Liao, J.-H.; Benz, M.; LeGoff, E.; Kanatzidis, M. G. *Adv. Mater.* **1994**, *6*, 135.
(49) DeWitt, L.; Blanchard, G. J.; Legoff, E.; Benz, M. E.; Liao, J. H.; Kanatzidis, M. G. *J. Am. Chem. Soc.* **1993**, *115*, 12158.
(50) Horne, J. C.; Blanchard, G. J.; LeGoff, E. *J. Am. Chem. Soc.* **1995**, *117*, 9551.
(51) Muguruma, H.; Kobiro, K.; Hotta, S. *Chem. Mater.* **1998**, *10*, 1459.
(52) Diaz-Quijada, G. A.; Weinberg, N.; Holdcroft, S.; Pinto, B. M. *J. Phys. Chem. A* **2002**, *106*, 1266.
(53) Dudek, M. J.; Ponder, J. W. *J. Comput. Chem.* **1995**, *16*, 791. Kong, Y.; Ponder, J. W. *J. Chem. Phys.* **1997**, *107*, 481. Kundrot, C. E.; Ponder, J. W.; Richards, F. M. *J. Comput. Chem.* **1991**, *12*, 402. Ponder, J. W.; Richards, F. M. *J. Comput. Chem.* **1987**, *8*, 1016.
(54) Leeflang, B. R.; Kroon-Batenburg, L. M. J. *J. Biomol. NMR* **1992**, *2*, 495.